Biosensors and Bioelectronics 288 (2025) 117836

Contents lists available at ScienceDirect

Biosensors and Bioelectronics

journal homepage: www.elsevier.com/locate/bios

Point-of-need one-pot multiplexed RT-LAMP test for detecting three common respiratory viruses in saliva

Aneesh Kshirsagar [a], Dean DeRosa [a], Anthony J. Politza [b], Tianyi Liu [a], Ming Dong [a], Weihua Guan [c,*]

[a] Department of Electrical Engineering, The Pennsylvania State University, University Park, PA, 16802, United States
[b] Department of Biomedical Engineering, The Pennsylvania State University, University Park, PA, 16802, United States
[c] Department of Intelligent Systems Engineering, Indiana University, Bloomington, IN, 47408, United States

ARTICLE INFO

Keywords:
Point-of-care
Multiplexed RT-LAMP
Respiratory virus detection
Saliva
Machine learning

ABSTRACT

Respiratory viral infections pose a significant global public health challenge, partly due to the difficulty in rapidly and accurately distinguishing between viruses with similar symptoms at the point of care, hindering timely and appropriate treatment and limiting effective infection control and prevention efforts. Here, we developed a multiplexed, non-invasive saliva-based, reverse transcription loop-mediated isothermal amplification (RT-LAMP) test that enables the simultaneous detection of three of the most common respiratory infections, severe acute respiratory syndrome coronavirus 2 (SARS-CoV-2), Influenza (Flu), and respiratory syncytial virus (RSV), in a single reaction via specific probes and monitored in real-time by a machine-learning-enabled compact analyzer. Our results demonstrate that the multiplexed assay can effectively detect three target RNAs with high accuracy. Further, testing with spiked saliva samples showed strong agreement with reverse transcription polymerase chain reaction (RT-PCR) assay, with area under the curve (AUC) values of 0.82, 0.93, and 0.96 for RSV, Influenza, and SARS-CoV-2, respectively. By enabling the rapid detection of respiratory infections from easily collected saliva samples at the point of care, the device presented here offers a practical and efficient tool for improving outcomes and helping prevent the spread of contagious diseases.

1. Introduction

The accurate diagnosis of respiratory infections is particularly challenging when multiple pathogens share similar clinical symptoms. Seasonal circulations of Influenza A (IAV), Influenza B (IBV), and Respiratory Syncytial Virus (RSV) were the most well-known examples of such viral infections until the widespread emergence of the Severe Acute Respiratory Syndrome Coronavirus 2 (SARS-CoV-2) virus(Olsen, 2021). These pathogens present similar or overlapping symptoms such as fever, cough, dyspnea, myalgia, and the typical changes in chest radiology images, including ground-glass opacities(Yang et al., 2022). As a result, healthcare providers may find it challenging to rely solely on syndromic diagnosis to pinpoint the exact causative pathogen, which may lead to delayed or purely symptomatic treatment(Bartlow et al., 2022). Inappropriate or insufficient treatment can lead to worsening symptoms or related complications, particularly in high-risk patient groups(Arons et al., 2020), resulting in longer recovery times and compromised outcomes(Beigel et al., 2020).

In addition, delays in accurate diagnosis can hinder public health measures such as infection control or quarantine protocols, potentially allowing the further spread of highly contagious pathogens. This challenge was particularly evident during the 2022–2023 US 'tripledemic' when widespread cases of SARS-CoV-2, Influenza, and RSV coincided, overwhelming clinics and hospitals(Furlow, 2023). Moreover, co-infection by two viruses has been reported worldwide (Cuadrado-Payán et al., 2020; Ding et al., 2020; Lansbury et al., 2020; Peci et al., 2021; Yue et al., 2020). Identifying and managing co-infections is crucial, particularly for high-risk cases, as different pathogens may require distinct treatments: remdesivir(Gottlieb et al., 2022), molnupiravir(Fischer et al., 2021), and nirmatrelvir co-formulated with ritonavir(Owen et al., 2021) for COVID-19, oral oseltamivir, inhaled zanamivir, or intravenous peramivir for Influenza (Stiver, 2003), and usually only symptomatic treatment for RSV(CDC, 2023). Thus, a reliable and timely molecular diagnosis of the causative agent(s) is essential to ensure that the most suitable treatment is administered within the appropriate window of 5–7 days for COVID-19

* Corresponding author.
E-mail address: guanw@iu.edu (W. Guan).

https://doi.org/10.1016/j.bios.2025.117836
Received 3 April 2025; Received in revised form 10 July 2025; Accepted 29 July 2025
Available online 30 July 2025

and 48 hours for Influenza after the onset of symptoms(Fischer et al., 2021; Stiver, 2003).

Current diagnostic practices to differentiate between infections often involve respiratory panels(Berry et al., 2022; Jarrett et al., 2021; Leung et al., 2021) that rely primarily on parallel polymerase chain reactions (PCR)(Mullis and Faloona, 1987) or isothermal amplification techniques such as loop-mediated isothermal amplification (LAMP)(Notomi et al., 2000), recombinase polymerase amplification (RPA)(Piepenburg et al., 2006), helicase-dependent amplification (HDA)(Vincent et al., 2004), or specific high-sensitivity enzymatic reporter unlocking (SHERLOCK) (Gootenberg et al., 2017), which may be conducted as sequential single-plex(Behrmann et al., 2020; C. Zhang et al., 2021; W. S. Zhang et al., 2021) or multiplex assays(Blumenfeld et al., 2022; Trick et al., 2022; Zhang and Tanner, 2021). While tests relying on nasal or nasopharyngeal (NP) swabs require careful collection by trained practitioners and could cause discomfort or increased risk of minor injury(Gagnon et al., 2022; Kim et al., 2022), anterior nasal (AN) swab-based tests such as those from Cue Health(Food and Drug Administration, 2024), Lucira (Pfizer Inc., 2023), Visby(Visby Medical, 2025), and Aptitude(Aptitude Medical Systems, 2025) have emerged as easier-to-administer options. Regardless of sample type, however, insufficient collection of genetic material can result in inconclusive or inaccurate results.

During the COVID-19 pandemic, saliva emerged as a promising and simplified alternative to nasal swabs for SARS-CoV-2 detection, offering comparable sensitivity even when stored without preservative reagents (Kudo et al., 2020; Ott et al., 2021; Vogels et al., 2021; Wyllie et al., 2020). In addition to SARS-CoV-2, saliva has been shown to contain detectable levels of other respiratory pathogens, including Flu-A/B and RSV. Studies have reported successful detection of Flu-A viral RNA in saliva with sensitivities comparable to that of NP swabs(Kim et al., 2016; To et al., 2017; Yoon et al., 2017), and RSV has similarly been detected in saliva in both pediatric and adult populations(Galar et al., 2021; Robinson et al., 2008). Saliva collection is non-invasive, easily self-administered, and generally well-tolerated, making it well-suited for molecular testing of respiratory infections, particularly in settings that prioritize ease of use, patient comfort, and frequent testing. Our previous work demonstrated a sample-to-answer test that uses saliva and reverse transcription loop-mediated isothermal amplification (RT-LAMP) to detect SARS-CoV-2 in a single-plex format with three parallel reaction chambers, which could be adapted for multiple targets (Tang et al., 2022). Other examples of direct RT-LAMP—i.e., minimal extraction-free sample preparation—for detection of SARS-CoV-2 from saliva include studies by Dewhurst et al. (2022); Kundrod et al. (2022); Lalli et al. (2021); Li et al. (2022). RT-LAMP often relies on non-specific detection methods such as intercalating dyes or colorimetric approaches, making multiplexing particularly challenging(Ball et al., 2016). Consequently, most studies detecting multiple targets rely on parallel reactions(Ackerman et al., 2020; Rombach et al., 2020; Yeh et al., 2017). While one-pot reactions offer advantages such as potentially improved sensitivity and eliminating the risk of non-uniform sample splitting, efforts to develop more specific detection strategies remain limited(Ball et al., 2016; Dong et al., 2022; Ludwig et al., 2021; Tanner et al., 2012). Notably, despite the growing demand for point-of-need tests, these strategies have not yet been widely implemented in such settings, which highlights a critical gap. Given RT-LAMP's potential and the ease of using saliva as a sample type, a one-pot point-of-need saliva-based nucleic acid test (NAT) leveraging isothermal amplification could enable large-scale adoption, home testing, and widespread screening for respiratory infections.

In this work, we developed a highly specific and multiplexed RT-LAMP-based test that utilizes saliva for the simultaneous detection of infections such as SARS-CoV-2, Influenza A (Flu-A), and RSV in a single reaction. The RT-LAMP assay uses the detection of amplification by release of quenching (DARQ) technique(Tanner et al., 2012) to allow multiplexed detection via fluorescently labeled primers specifically for a target. Complementing this assay, we developed a compact, battery-powered instrument capable of detecting multiple fluorophores simultaneously, empowered by machine learning to estimate time-varying fluorophore concentrations. In contrast to traditional systems with excitation and emission filters, which may limit the number of detectable targets, our design does not rely on expensive optical filters for specificity and eliminates the need for hardware reconfiguration when incorporating new or additional fluorophores, allowing for easy future adaptation to new pathogens or variants. We demonstrate the assay's potential to address the critical need for differentiating between respiratory infections and identifying co-infections by running the optimized multiplexed RT-LAMP assay on mock saliva samples spiked with single or combinations of target RNAs. This system can potentially enhance diagnostic efficiency, enabling the more precise identification of co-infections and pinpointing the causative pathogens in point-of-need settings, thereby improving timely treatment decisions and patient outcomes.

2. Materials and methods

Please see the supplementary information for details.

3. Results

3.1. A saliva-based point-of-need diagnostic test for multiplexed respiratory tri-virus detection

To accurately identify the possible causative virus leading to respiratory symptoms at the point of need, we propose a diagnostic test, the workflow of which is given in Fig. 1a. It involves the collection of saliva, extraction of RNA using the Qiagen RNA extraction mini kit performed on a custom-developed potable centrifuge, and finally, running the one-pot multiplexed RT-LAMP reaction on a portable nucleic acid testing device while using all the relevant primer sets and distinct fluorescent probes to distinguish between SARS-CoV-2, Flu-A, RSV or no infection.

To allow one-pot multiplexing, we make use of distinct fluorophores for each viral target, and Fig. 1b schematically outlines the DARQ RT-LAMP mechanism, which allows multiplex detection via fluorescently labeled probes, initially described by Tanner et al. (2012). Like traditional LAMP, DARQ LAMP consists of six primers that target eight regions of the template cDNA with the Forward Internal Primer (FIP) tagged with a quencher on the 5' end (termed QFIP) and a corresponding probe complementary to only the F1c region and tagged with a fluorophore (termed Fd). Fd and QFIP are annealed together by heating to 95 °C and slowly cooling to room temperature at ~1 °C/min in a controlled manner before adding to the amplification reaction. Like traditional LAMP, DARQ LAMP initiates at the F2c region while the fluorescent probe remains annealed and quenched. This strand is then displaced because of the hybridization of the F3 primer to initiate a new strand. Meanwhile, the previously displaced strand experiences hybridization at the B2c region, and upon extension, the annealed Fd is released from QFIP to produce fluorescence. As LAMP progresses, more amplicons are generated to produce more fluorescence until a plateau is reached. Please note that the reverse transcription step and other intermediate steps within LAMP are not shown for simplicity.

The one-pot reaction is performed on a handheld analyzer, iNAAT, and Fig. 1c presents its 3D render. The three main modules of the developed analyzer are detailed in Supplementary Fig. S1a. The analyzer is designed to run eight reactions in parallel, is compatible with traditional PCR tubes, and has a power consumption of ~5 Wh such that it can be powered either by a commercial rechargeable battery pack to allow up to 12 hours of in-field use, or by a wall adapter to allow potentially continuous lab use. iNAAT integrates a compact and modular optical assembly designed for flexible and scalable fluorescence-based multiplexing without hardware reconfiguration. The system utilizes an RGB LED (SK6812) as a tri-wavelength excitation source and a CMOS spectral sensor (AS7341) as the emission detector, both mounted

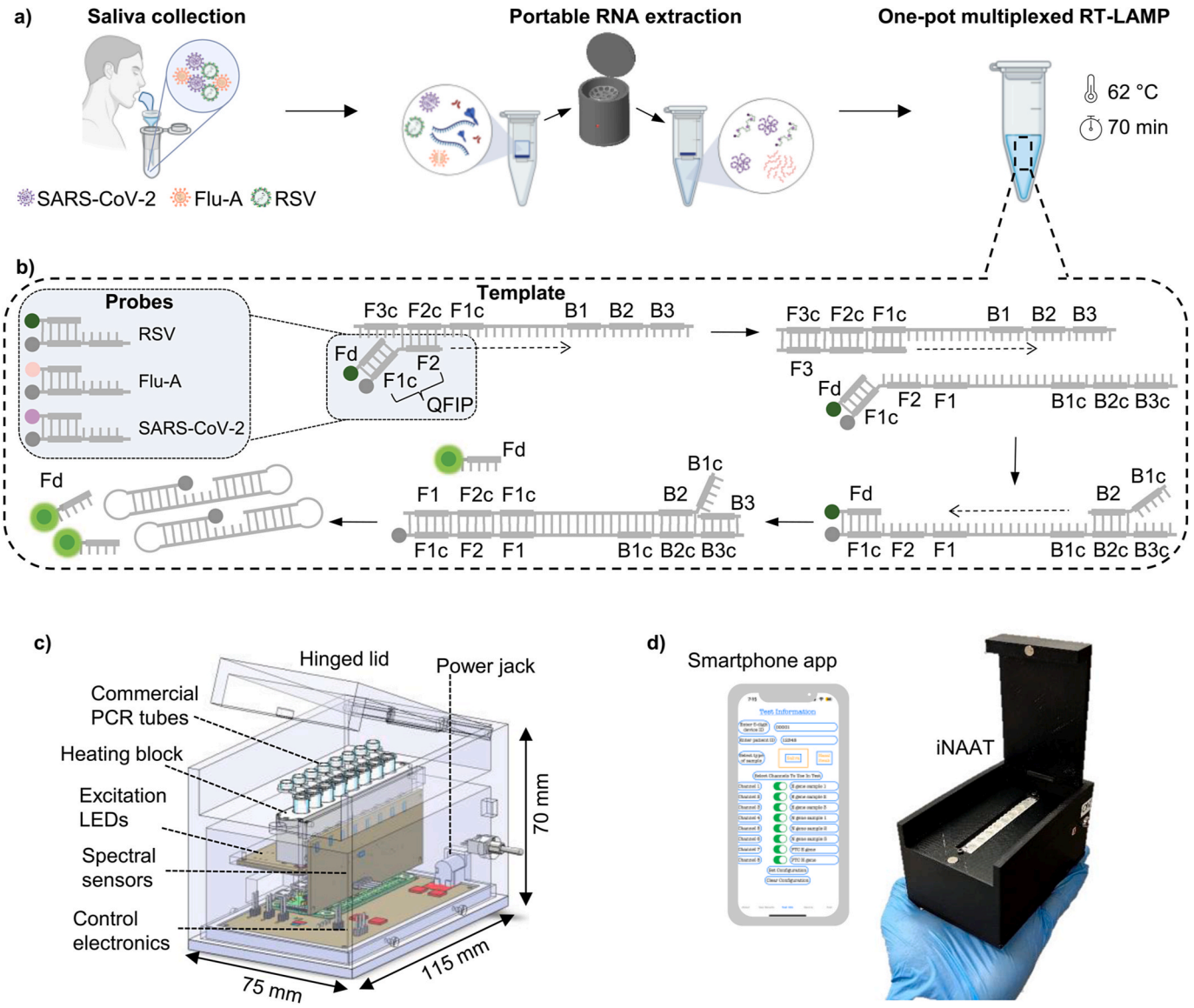

Fig. 1. An overview of the test and the analyzer developed for multiplexed monitoring of RT-LAMP reaction. (a) The test workflow involves i) saliva collection, ii) portable RNA extraction, and iii) multiplexed RT-LAMP using specific primers and distinct fluorescent probes, enabling one-pot multiplexing. Multiplexing allows simultaneous detection and differentiation of RSV, Flu-A, SARS-CoV-2, or no infection within a single reaction. (b) Schematic representing the mechanism of DARQ RT-LAMP for multiplex detection using fluorescently labeled probes. A quencher-tagged Forward Internal Primer (QFIP) is annealed to a fluorescently labeled probe (Fd) complementary to the F1c region before adding it to the reaction. The fluorescent probe remains quenched during initiation at the F2 region, and subsequent displacement of the quenched strand is triggered by the hybridization of the F3 primer, leading to fluorescence release as the Fd probe separates from QFIP when the Backward Internal Primer (BIP) initiates backward strand formation. Fluorescence production increases as more amplicons are generated during LAMP until a plateau is reached. (c) 3D CAD diagram of the developed analyzer, which can run up to eight multiplexed reactions in parallel and is compatible with traditional PCR tubes. (d) Pictorial representation of the fabricated analyzer and a smartphone running the custom-developed app.

orthogonally without the use of lenses. The spectral sensor captures emission across eight discrete channels in the visible spectrum, enabling real-time fluorescence measurements over a broad emission range. Reactions (containing mixtures of fluorescent probes) are sequentially excited using the LED's blue, green, and red sources, and emissions are recorded across all eight channels to generate 24 features (fluorescence signatures). These collective emissions are analyzed using a supervised machine learning model—specifically, a neural network trained on calibration data from known fluorescent probe mixtures—to deconvolute overlapping emission spectra and predict concentrations in unknown samples. This approach allows simultaneous, quantitative readout of multiple target-specific probes in a single reaction and supports rapid reconfiguration by retraining the model without altering hardware components. A detailed description of the optical system, calibration procedure, and machine learning pipeline is provided in our prior publication(Kshirsagar et al., 2024).

The predicted concentrations are shared with an iOS app over Bluetooth, developed to provide test instructions, acquire data, and make positive and negative calls to interpret the test results. Fig. 1d shows the in-house fabricated analyzer and a smartphone running the app, and **Supplementary Video V1** demonstrates the test workflow. While portable isothermal devices, such as the BioRanger (Diagenetix Inc., 2025) and WeD from EzDx (Dai et al., 2025), support field-deployable fluorescence detection, they rely on fixed optical channels and lack demonstrated scalability for multiplexed analysis. Our analyzer supports software-driven multiplexing through machine learning-based spectral deconvolution, eliminating the need for hardware modifications.

Supplementary video related to this article can be found at https://doi.org/10.1016/j.bios.2025.117836

3.2. DARQ RT-LAMP assays' cross-reactivity validation

To develop a multiplexed RT-LAMP assay, we first verified that each of the primer sets targeting RSV, Flu-A, and SARS-CoV-2 is specific, i.e., does not detect any of the other targets and does not interact with each other to form primer dimers that may lead to false amplification. Fig. 2a shows the specific regions of the three RNA targets that are amplified and detected during the single-plex DARQ RT-LAMP reactions, N, HA, and N1, for RSV, Flu-A, and SARS-CoV-2, respectively. The primer sequences used in these assays have been previously reported(Broughton et al., 2020; Takayama et al., 2019; Zhang and Tanner, 2021), with modifications made to the FIP, incorporating a quencher at the 5′ end (QFIP), and designing a complementary fluorescence labeled Fd probe. These primer and probe sequences are listed in Supplementary Table 1. A preliminary inspection of all the sequences using online tools such as NCBI BLAST, IDT's Oligo Analyzer, and ThermoFischer's Multiple Primer Analyzer did not indicate any non-target amplification and any significant probability for false amplification due to primer-primer interaction or primer-dimer formations.

To verify this experimentally, we conducted cross-reactivity tests for the single-plex assays on a benchtop thermal cycler. To test cross-reactivity, we ran the DARQ RT-LAMP assays using 1000 copies per reaction (cp/rxn) of RSV, Flu-A, and SARS-CoV-2 RNAs as input targets separately. The normalized amplification curves (triplicates) for all combinations (three assays and four targets, each including water as the

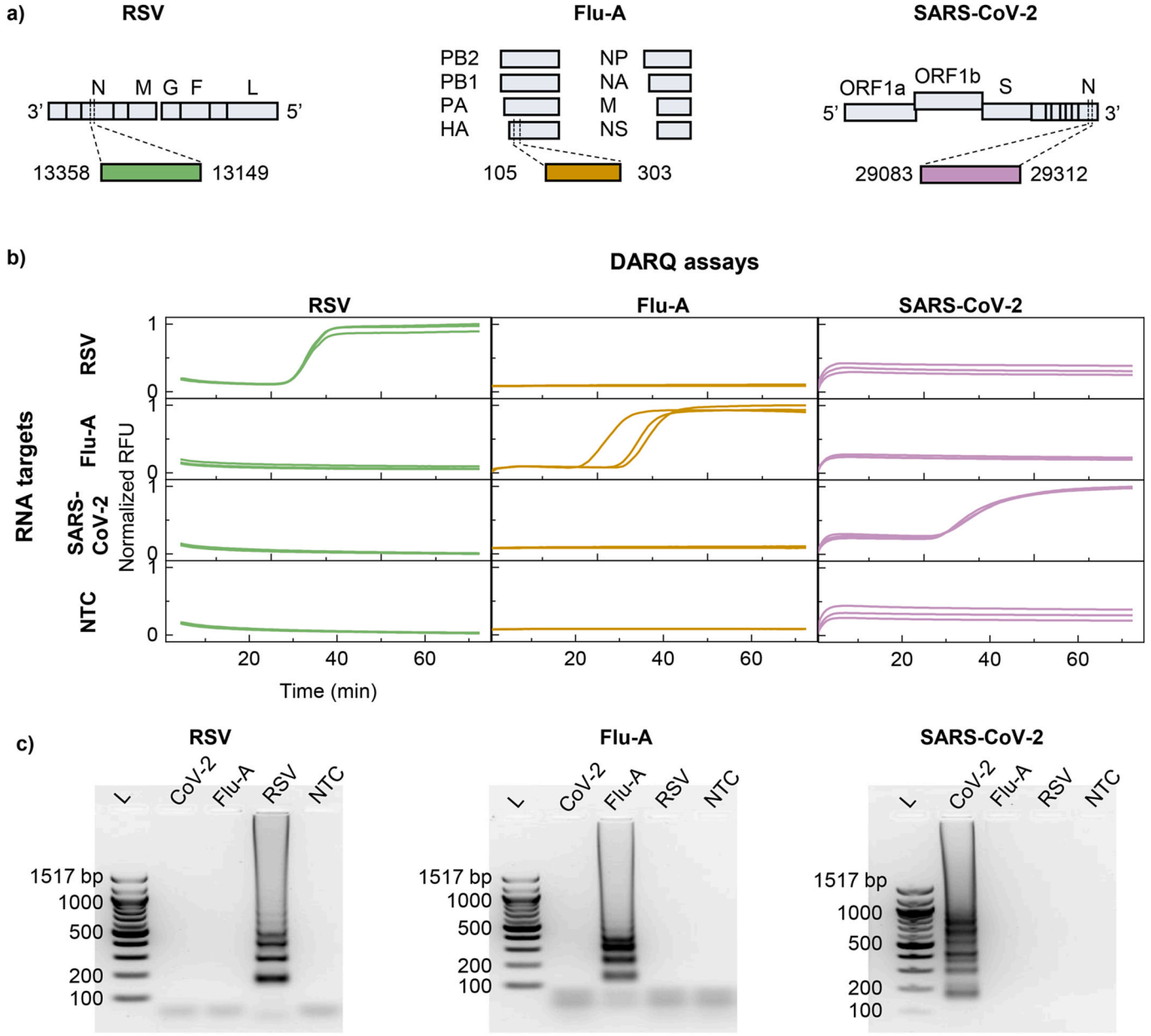

Fig. 2. Preliminary validation of the DARQ RT-LAMP primer sets. (a) Specific regions of the three RNA targets that are amplified and detected during the single-plex DARQ RT-LAMP reactions, N, HA, and N1 for RSV, Flu-A, and SARS-CoV-2, respectively. Modifications were made to previously reported FIPs, incorporating a quencher at the 5′ end (QFIP) and adding a complementary fluorescence-labeled Fd probe to the reaction mix. (b) The normalized amplification curves (triplicate) present the results of cross-reactivity tests for the DARQ RT-LAMP single-plex assays for 1000 cp/rxn of RSV, Flu-A, and SARS-CoV-2 RNAs as input targets separately and NTC on a benchtop thermal cycler. The matrix of amplification curves shows no cross-reactivity. (c) Images of gel electrophoresis performed on reaction products from subfigure b. The ladder patterns, visible only for the intended targets in the case of all three assays, corroborate the real-time results.

negative control) are displayed as a matrix in Fig. 2b. Amplification curves only along the diagonal of the matrix suggest only specific amplification of the intended RNA target for all assays, without any false positives. This confirms the specificity of each assay, demonstrating no cross-reactivity with other target sequences, and serves as a fundamental validation of assay specificity. It may be noted that for some conditions testing the specificity of the SARS-CoV-2 assay, the replicate curves do not completely overlap. However, since these results are used only to evaluate cross-reactivity, and the experiments were performed on a benchtop thermal cycler and not used for any further analysis, we do not expect them to influence the limit of detection values determined further using separate experiments performed on the developed instrument.

As a confirmatory test, we subjected all the reaction products to gel electrophoresis, and the results of all the assays are shown in Fig. 2c. Ladder patterns, visible only for the intended targets in the case of all three assays, corroborate the real-time results. However, the use of DARQ primers may reduce early amplification efficiency due to the need for dissociation of the fluorophore-quencher duplex and possible steric hindrance from the quencher itself, which can interfere with primer-template hybridization, polymerase access, and loop structure formation. These factors can limit the formation of recursive, self-primed amplicons critical for exponential signal generation in LAMP. Tanner et al., 2012 demonstrated that DARQ duplex primers delay amplification onset, with time-to-threshold increasing approximately twofold. In our results, fewer distinct rungs are observed, and higher-molecular-weight bands appear fainter. This variation from the typical LAMP ladder may stem from reduced efficiency of early amplification events and limited loop structure formation due to DARQ primers, resulting in less concatemer diversity and attenuated propagation of longer products. Nonetheless, these results confirm that none of the assays show any cross-reactivity for the targets considered in this study and may be used further for a multiplexed detection assay.

3.3. Performance of single-plex DARQ RT-LAMP assays on the analyzer

After confirming the absence of cross-reactivity in the DARQ assays against non-target RNAs, we evaluated the individual performance of each DARQ RT-LAMP assay by attempting to detect serially diluted

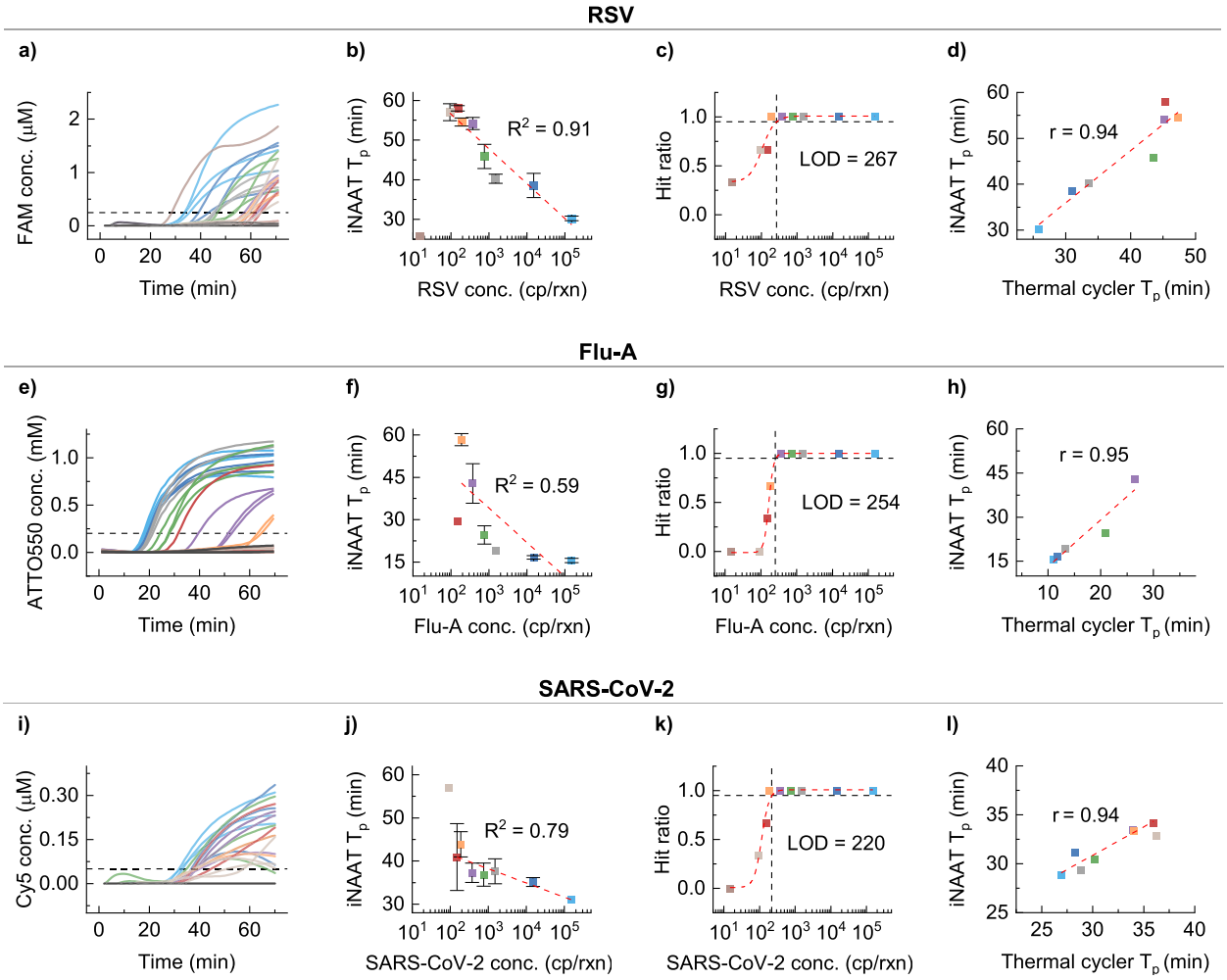

Fig. 3. Analytical characteristics of the DARQ assays performed on the analyzer. (a) Amplification curves for the RSV assay, spanning a range of serially diluted RSV RNA concentrations, 10x serial dilution between $1.5x10^5$ and 15 copies/rxn, followed by 2x serial dilution between 750 and 93.75 copies/rxn. The horizontal dashed line represents the threshold concentration computed as $\mu+3\sigma$, where μ is the mean, and σ is the standard deviation for NTC reactions. (b) Summary of the time to positive (T_p) for triplicate reactions at each RNA concentration with a linear fit of $R^2 = 0.91$. (c) The hit ratio for these serially diluted samples and a logistic fit reveal a limit of detection of 267 copies/rxn. (d) A scatter plot comparing the T_p values measured on the analyzer with those measured on a benchtop thermal cycler suggests good collinearity, with a Pearson's r value of 0.94. (e), (f), (g), and (h) present the same information for the Flu-A DARQ assay and reveal that the linear response between T_p and RNA concentration has $R^2 = 0.59$ with a LOD of 254 copies/rxn, and collinearity with thermal cycler has a Pearson's $r = 0.95$. (i), (j), (k), and (l) present the performance of the SARS-CoV-2 assay that has a linear response between T_p and RNA concentration with $R^2 = 0.79$ and LOD of 220 copies/rxn, and collinearity with thermal cycler has a Pearson's $r = 0.94$.

target RNA on both the developed analyzer and a benchtop thermal cycler parallelly. We used target RNAs in the range $1.5x10^5$ to 15 cp/rxn with 10x dilution and then in the range 750 to 93.75 cp/rxn with 2x dilution in triplicate reactions for all concentrations in the RSV, Flu-A, and SARS-CoV-2 assays. The results for baseline-subtracted amplification curves for the RSV assay obtained on the analyzer are presented in Fig. 3a. The threshold line (black dotted) is calculated such that $C_{th} = \mu + 3\sigma$, where μ and σ are the mean and standard deviation of the predicted fluorophore concentration for the NTC reactions. This threshold concentration was calculated separately for each assay to measure the times to positive (T_p) for all reactions that showed amplification. The mean times to positive as a function of RNA concentration are shown in Fig. 3b, with a linear fit having an R^2 value of 0.91.

To estimate the LOD of the assay, we examined the hit ratios at various RNA concentrations, which are given as the number of positive tests over the total number of tests at a particular concentration and presented in Fig. 3c. The experimental hit ratio data was fit with a logistic curve to reveal the LOD as 267 at the 95 % confidence level when 1.5 μL RNA was used in a 25 μL reaction. However, considering an estimated concentration of ~8.4×10^7 cp/mL of RSV in nasal washes (Perkins et al., 2005) and assuming a conservative 10-fold reduction in saliva, we estimate ~8.4×10^6 cp/mL in raw saliva. RNA extraction from 200 μL of sample, elution into 60 μL, and accounting for ~85 % recovery efficiency would yield ~1700 cp/μL in the eluate. Using 1.5 μL per reaction, this corresponds to ~2500 cp/rxn, which should be sufficient for qualitative detection in a multiplexed assay. Fig. 3d compares the times to positive seen on the analyzer and a benchtop thermal cycler at various concentrations. A Pearson's r value of 0.94 for RSV suggests that the analyzer's operation is independent of the assay, and the efficiency and LOD observed are assay artifacts not affected by the analyzer. Please refer to Supplementary Fig. S2 for the amplification reactions performed on the benchtop thermal cycler.

Similarly, Fig. 3e–h presents the performance of the Flu-A assay with a linearity (R^2) of 0.59, a LOD of 254 cp/rxn, and a Pearson's r of 0.94 when benchmarking the analyzer against a benchtop thermal cycler. Considering an estimated concentration of ~$3.1x10^6$ cp/mL for Flu-A (Ngaosuwankul et al., 2010) in clinical samples, it should be sufficient. Fig. 3i–l presents information for the SARS-CoV-2 assay, which has a linearity (R^2) of 0.79, a LOD of 220 cp/rxn, and a Pearson's r of 0.91, considering ~10^7 cp/mL for target RNA in SARS-CoV-2 samples

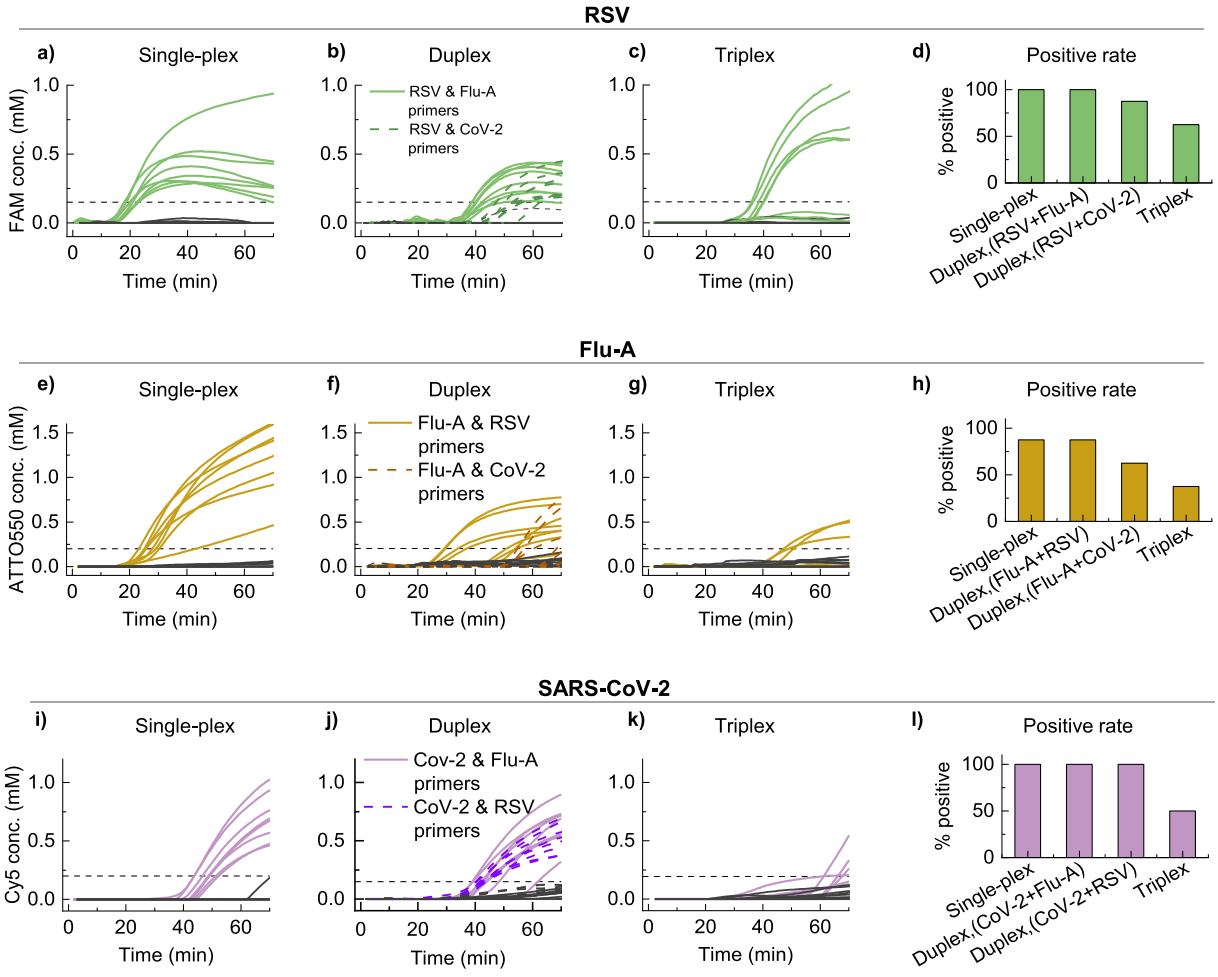

Fig. 4. Evaluating the effect of increasing the number of distinct primer sets on the detection of a target RNA. (a), (b) and (c) Present the amplification curves of the single-plex, duplex, and triplex assays when 750 copies/rxn of RSV RNA (green) and negative controls (dark gray) were added as input to the reaction in eight replicates. (d) The positive detection rate for all assays when targeting RSV. (e), (f) and (g) Present the amplification curves for the same set of primers as in a, b, and c when 750 copies/rxn of Flu-A RNA (yellow) and negative controls (dark gray) were added as input. (h) The positive detection rate for all assays when targeting Flu-A. (i), (j), and (k) Present the amplification curves for 750 copies/rxn of SARS-CoV-2 RNA (purple), and negative controls (dark gray), added as input. (l) The positive detection rate for all assays when targeting SARS-CoV-2. In general, the detection rate decreases for all targets as the number of primer sets increases, even with minimal assay optimization. This is likely due to a reduction in the concentration of the primers that target the specific RNA when the primer sets are multiplexed together to keep the total primer concentration commensurate with the amount of DNA polymerase. (For interpretation of the references to color in this figure legend, the reader is referred to the Web version of this article.)

(Faruque et al., 2023), this LOD would be sufficient. Although these results indicate a semi-quantitative ability and demonstrate varying efficiencies for each assay, they show the performance of the single-plex assays, the analyzer's ability to amplify target RNAs, and its comparable performance to a benchtop thermal cycler. However, this finding is not expected to impact the qualitative detection capabilities of the subsequent multiplexed assay, which is the goal of this study.

3.4. Effect of multiplexing DARQ assays on the detection of a single RNA target

After evaluating the single-plex assay performances, we set out to test the impact of multiplexing the primer sets on detecting a single RNA target of fixed concentration. We attempted to amplify 750 cp/rxn of RSV, Flu-A, and SARS-CoV-2 purified RNAs independently using the single-plex, duplex, and triplex assays. To depict the outcomes of these experiments, the baseline-subtracted amplification curves of eight replicates for the positive and negative control reactions under different primer set conditions are shown in Fig. 4a–c.

When multiplexing primer sets together, certain assay parameters needed optimization to prevent false positives due to increased primer-primer interaction and to enable enzyme activity similar to the single-plex assay. For the duplex assay in Fig. 4b, the primer concentrations were reduced to 50 % of the concentrations used in the single-plex assay (Fig. 4a). Similarly, for the triplex assay (Fig. 4c), the primer concentrations were reduced to 33 % of the single-plex assay concentrations, or 1/n of the usual concentration, where n is the number of primer sets in the multiplexed assay. Another condition that was optimized was the ratio of FIP:QFIP, which was changed to ~1.5:1 instead of 1:1. Thus, the minimal assay optimization helped preserve the detection ability for RSV targets as the degree of multiplexity increased up to three, albeit poor efficiency as evidenced by the reducing number of reactions containing target showing amplification. A summary, presented in Fig. 4d, shows that plotting the percentage positive rate for the detection of RSV RNA in the presence of different primer sets reveals a decrease in the detection rate as more primer sets are added.

On the same lines, the detection rates of Flu-A (Fig. 4e–h) and SARS-CoV-2 (Fig. 4i–l) also decreased as the number of primer sets added to the assay increased, most likely due to the reduced primer concentrations. While slight differences in detection rates across targets exist, the triplex assay demonstrated clear detection capability for RSV, Flu-A, and SARS-CoV-2 replicates. These results show that although the sensitivity of detection for each target may be affected due to the reduced primer concentrations, no false positives resulting from primer-primer interaction were observed in any of the multiplexed assays. Consequently, the triplex assay can be used for detecting multiple targets in the same reaction.

3.5. Triplex assay to detect multiple RNA targets

In the previous section, we demonstrated the adverse effect of increasing the number of primer sets on detecting a single RNA target of fixed concentration due to the reduced concentrations of individual primers. This section evaluates the triplex assay's ability to detect multiple RNA targets simultaneously, simulating a situation where a patient may have a co-infection of two or more respiratory pathogens. Since any fluorophore (attached to the specific probe) has an emission spectrum rather than emission at a single wavelength, multiple channels of the spectrophotometer may detect this emission, and the emission spectra from multiple fluorophores in a reaction tube may overlap, preventing an easy readout. To resolve these overlapped emission spectra, we developed a Multilayer Perceptron (MLP) Neural Network to predict the time-varying fluorophore concentration of the triplex RT-LAMP assay(Kshirsagar et al., 2024).

The triplex assay was used to detect 1500 cp/rxn of each RNA target in eight different combinations: individual targets, two targets, all three targets, and NTC. The raw fluorescence data acquired by the analyzer was fed to the NN to predict the time-varying fluorophore concentrations for the progressing reaction. The predicted fluorophore concentrations for eight replicates of each combination are presented as real-time amplification curves for RSV, Flu-A, and SARS-CoV-2 in Fig. 5a–c, respectively. Although no clear trend was observed among times to positive, even if multiple targets are present and accurately detected by the triplex assay, we noticed certain false positives and negatives for each target.

The assay's detection ability is summarized in Fig. 5d using a binary comparison plot, which compares the presence or absence of input RNA targets (RSV, Flu-A, and SARS-CoV-2) with the assay's detection results. This figure visually represents whether the assay successfully detected the input target RNA for each sample, highlighting its ability to identify single or multiplexed targets. Further illustrating the assay's performance, Fig. 5e presents a confusion matrix that quantifies the number of correct target-wise classifications, ranging from zero to eight, across different RNA combinations. The overall classification accuracy of the assay is 80 %, with the highest number of misclassifications observed for the combination that contains all three RNAs simultaneously. This may suggest variability in amplification kinetics across combinations and preferential amplification of certain targets, leaving insufficient resources for others. Thus, this figure demonstrates the ability of the triplex assay to detect all RNA targets, whether present individually or in combination with another target, and it can be used for multiplexed and co-infection detection.

3.6. Spiked saliva sample testing

After validating that the triplex assay can detect single and multiple targets using the respective purified RNAs, we attempted to detect single and co-infections in mock saliva samples. The mock samples were prepared by spiking purified RNA in negative saliva obtained from volunteers such that each target was present at a clinically relevant concentration of $5x10^5$ cp/mL of saliva. 200 μL of such spiked saliva was used to extract and purify the viral RNA using the Qiagen QIAamp viral RNA mini kit and a portable centrifuge to elute a final volume of 60 μL. In a separate work, we have demonstrated the use of this custom-developed portable centrifuge (Politza et al., 2024) with an ~85 % efficiency for use with a column-based extraction kit and a performance comparable to a benchtop centrifuge. Thus, we expect a viral RNA concentration of ~1400 cp/μL of eluate from 200 μL of raw saliva and ~6300 cp/rxn when 4.5 μL eluate is used in each triplex reaction.

After verifying satisfactory RNA extraction, the 14 mock samples having one, two, or no RNA targets were tested using single-plex RT-PCR (triplicate) as a gold standard. The amplification curves for RSV, Flu-A, and SARS-CoV-2, shown in Supplementary Fig. S3, indicate accurate identification and quantification of the target RNA in each mock sample. Then, the same samples were tested using the triplex RT-LAMP assay in triplicate. Fig. 6a–c shows the predicted fluorophore concentrations representing the real-time amplification curves for each target of the triplex assay. Binary comparison plots in Fig. 6d show that the triplex RT-LAMP assay classification matched with RT-PCR for 32 out of 42 tests (14 mock samples tested in triplicate), i.e., 76 % agreement. This is further summarized by plotting the receiver operating characteristic (ROC) curves for each target separately in Fig. 6e–g, and the area under the curve (AUC) values are 0.82, 0.93, and 0.96 for RSV, Flu-A, and SARS-CoV-2, respectively. Thus, this section demonstrates the ability of the DARQ triplex assay to qualitatively identify single or co-infection of RSV, Flu-A, or SARS-CoV-2 targets in saliva samples using a single reaction on the portable analyzer, and is fully ready to be implemented at the point of need. Please note that we did not attempt the detection of three targets in saliva, as it would be a highly improbable situation where a patient is infected with three different viruses at the same time; however, the previous section provides sufficient evidence that this triplex test would be able to identify it as well.

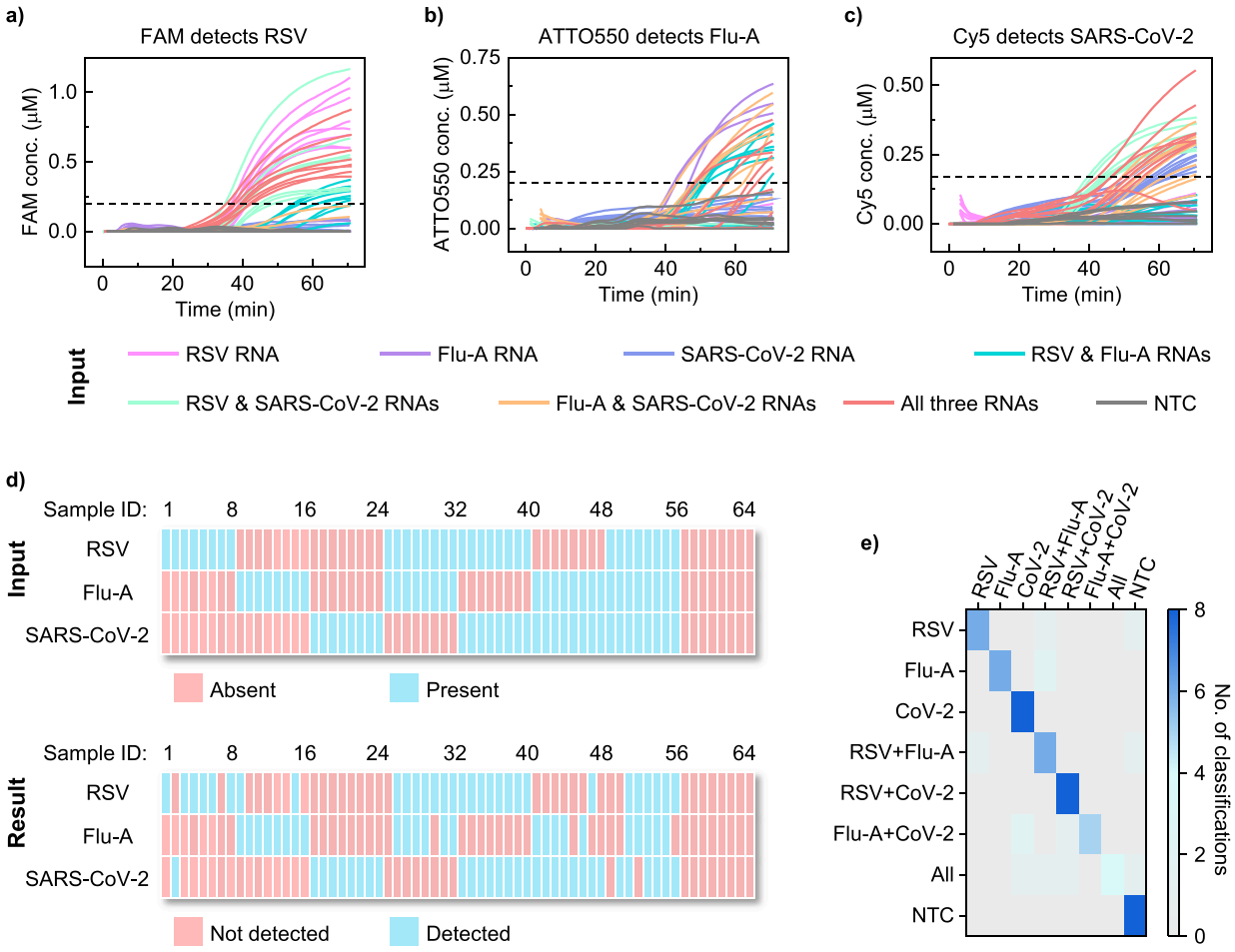

Fig. 5. The ability of the triplex DARQ RT-LAMP assay to correctly classify single or combinatorial purified RNA input. (a) The amplification curves for detection of RSV RNA marked by the FAM fluorophore for various (eight) scenarios, including single RNA targets, dual RNA targets, all RNA targets (concentration: 1500 cp/rxn), and NTC. The horizontal dashed line represents the threshold concentration computed as μ+3σ, where μ is the mean, and σ is the standard deviation for NTC reactions. (b) The amplification curves for detection of Flu-A RNA marked by the ATTO550 fluorophore for the same reactions as in a. (c) The amplification curves for detection of SARS-CoV-2 RNA marked by the Cy5 fluorophore for the same reactions as in a. (d) Binary comparison plot between input RNA targets and assay detection results. The top panel represents the input matrix, showing the presence or absence of RSV, Flu-A, or SARS-CoV-2 RNA in each sample (eight replicates for eight scenarios). The bottom panel displays the detection results from the triplex DARQ RT-LAMP assay. Blue indicates presence/detection, while pink represents absence/non-detection. (e) Confusion matrix summarizing the assay's classification accuracy, where each cell represents the number of classifications for a specific combination of input RNA targets (range: zero to eight). This demonstrates the assay's ability to accurately detect single and multiplexed RNA targets, with an overall detection accuracy of 80 %. (For interpretation of the references to color in this figure legend, the reader is referred to the Web version of this article.)

The method used for RNA extraction can indeed influence the LOD of any diagnostic system. Common approaches include silica column-based extraction, magnetic bead-based isolation, heat inactivation, detergent-assisted lysis with stabilizers, and phenol–chloroform extraction. Each varies in RNA yield, inhibitor removal, and compatibility with amplification. Our prior studies have evaluated simplified methods such as magnetic bead-based(Liu et al., 2022; Politza et al., 2023), heat-inactivation(Z. Tang et al., 2022), and detergent-based methods(Kshirsagar et al., 2023) for field-deployable applications. While these offered simplified and integrated workflows, they lacked RNA concentration or purification step, resulting in lower recovery and increased the risk of amplification inhibition from carried-over matrix components. Silica column-based extraction using our portable centrifuge offers a practical and field-deployable solution that combines robust RNA recovery with effective inhibitor removal through multiple wash steps. It ensures compatibility with downstream amplification while retaining portability and reliability, making it a suitable choice for clinical and point-of-need use. For this extraction method, viral RNA concentrations in saliva were estimated based on prior studies that reported typical respiratory viral RNA loads. Estimated concentrations include approximately $8x10^7$ cp/mL for RSV, assuming 150 RNA copies per plaque-forming unit equivalents (PFUe) (Perkins et al., 2005), $3x10^6$ cp/mL for Flu-A(Ngaosuwankul et al., 2010), and 10^7 cp/mL for SARS-CoV-2(Faruque et al., 2023). Considering RNA is extracted from 200 μL of saliva and eluted into 60 μL using our portable centrifuge with ~85 % efficiency, the eluate is expected to contain $2.8x10^4$ to $2.4x10^5$ cp/μL. Using 4.5 μL of eluate per reaction, this corresponds to $1.3x10^5$ to $1.1x10^6$ cp/rxn in the triplex assay. These estimates confirm that the conservative concentration ($5x10^5$ cp/mL) used in the mock samples accurately reflects clinically relevant viral loads. The observed performance of the triplex assay further supports the suitability of the chosen RNA extraction method for clinical and point-of-need applications.

4. Discussion

Point-of-need tests for respiratory symptoms should ideally be minimally invasive, provide rapid sample-to-answer results, and be easy to administer. This approach allows for quick differentiation between infections with similar symptoms while reducing patient hesitance and minimizing the risk of injury. A prompt diagnosis also enables timely,

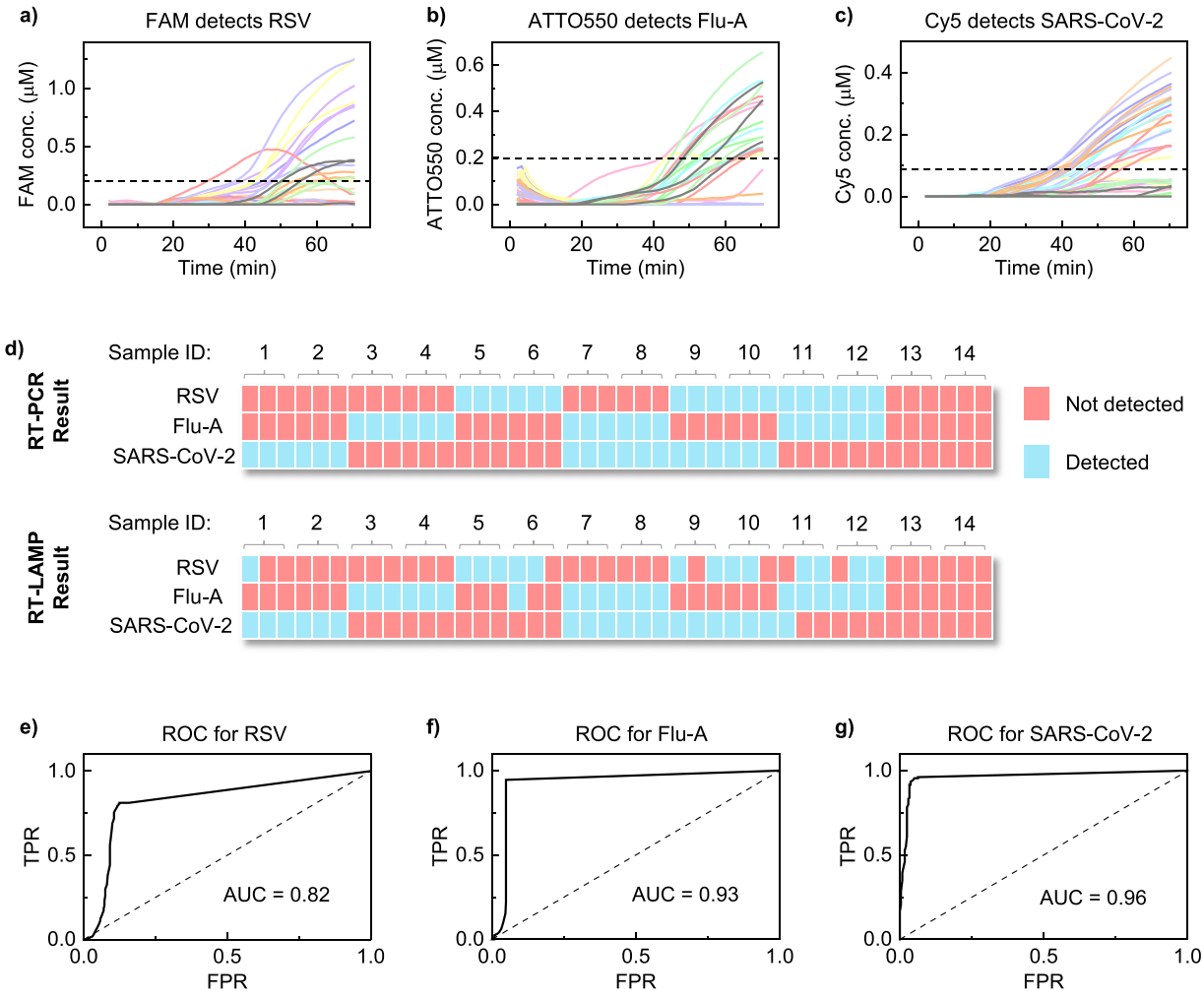

Fig. 6. Mock saliva sample testing using the developed triplex RT-LAMP assay. Mock saliva samples were prepared by spiking purified RNA in negative saliva obtained from volunteers such that each target is present at a clinically relevant concentration of $5x10^5$ cp/mL of saliva. (a), (b) and (c) Present the real-time amplification curves for detecting RSV, Flu-A, and SARS-CoV-2 by the triplex DARQ RT-LAMP assay on the analyzer. (d) Binary comparison plot demonstrating 76 % agreement (as per strict exact match criteria) between the triplex RT-LAMP assay and RT-PCR when 14 mock samples were tested in triplicate. (e), (f) and (g) display the Receiver Operating Characteristic (ROC) curves for RSV, Flu-A, and SARS-CoV-2, respectively, comparing the performance of triplex RT-LAMP against single-plex RT-PCR as the ground truth. TPR: True Positive Rate, FPR: False Positive Rate.

targeted treatment within optimal therapeutic windows, enhancing effectiveness. Conducting a panel of targets in such multiplexed tests on saliva enables the simultaneous detection of multiple pathogens, including co-infections, thereby further supporting comprehensive and accurate diagnosis.

In this work, we developed a multiplexed diagnostic test designed to detect SARS-CoV-2, Flu-A, and RSV RNA from non-invasive saliva samples, directly addressing the challenge of distinguishing between respiratory viral infections with overlapping symptoms at the point of need. Our approach tackles the issue of differentiating overlapping spectral signals from multiple fluorophores within the same reaction tube by first gathering calibration data for fluorophore combinations and then training a neural network model to estimate time-varying fluorophore concentrations in a multiplexed RT-LAMP assay using a simple, low-cost device that does not rely on specialized optical filters, unlike other examples(Blumenfeld et al., 2022; Xun et al., 2021). Future efforts will focus on refining the neural network model to leverage calibration data from individual fluorophores, which could enable the model to predict the combined behaviors of fluorophores, thereby reducing the need for extensive combinatorial experiments.

LAMP assays are vulnerable to false positives arising from two primary sources: non-template amplification, where primers amplify themselves in the absence of target nucleic acid, and non-specific amplification, where unintended sequences in the sample are amplified. These artifacts can be exacerbated in multiplexed assays due to the high number of unique primer sequences and increased risk of primer–primer interactions. To mitigate these effects, we adopted the DARQ strategy described by Tanner et al. (2012). In DARQ, the Forward Inner Primer (FIP) is modified with a 5' quencher (QFIP) and annealed to a fluorophore-labeled probe (Fd) that binds the F1c region. This duplex remains quenched unless it is correctly displaced during template-specific strand displacement by the DNA polymerase. As a result, fluorescence is only generated when true target amplification occurs, effectively distinguishing signal from background amplification events. Unlike traditional LAMP, where any DNA synthesis may produce signal through intercalating dyes or turbidity, DARQ restricts signal generation to authentic, sequence-specific events.

Additionally, we adopted their recommendation to reduce the concentration of each primer set to 1/n of the single-plex version (where n is the number of targets in the multiplexed version) to minimize non-template artifacts while maintaining a total primer concentration comparable to that of single-plex LAMP. The absence of false positives in the

purified RNA tests and the low incidence of false positives in mock saliva tests demonstrate the analytical specificity of our triplex RT-LAMP assay. While we did not experimentally compare false-positive rates under alternate assay conditions, the DARQ probe system and primer concentration adjustments were intended to simplify assay design and minimize non-template amplification and spurious signal. This approach enhances the reliability of results, which is essential for accurate pathogen screening. However, the observed reduction in positivity rate indicates a trade-off in sensitivity as multiplexing increases.

Despite the design optimizations described above, multiplexed reactions in our system exhibited certain atypical amplification features that warrant further discussion. These include rising baselines, biphasic amplification, and in some cases, gradual decreases in fluorescence signal. Such features have been observed in prior reports using DARQ or other probe-based LAMP systems(Hardinge and Murray, 2019; Tanner et al., 2012; Zhang and Tanner, 2021), and likely result from a combination of factors. Lower per-target primer concentrations, adopted to keep the overall concentration consistent with typical LAMP, may prolong the early phase of amplification before sufficient templates accumulate to initiate exponential growth. In parallel, DARQ requires the dissociation of the Quencher-Probe Duplex (QPD) before fluorescence is observed. Partial duplex dissociation and competition between QFIP and standard FIP primers can delay signal release, resulting in gradual baseline increases or biphasic curves. Competition for shared reaction components such as dNTPs and polymerase may also contribute, especially when differences in target abundance or primer binding efficiency lead to uneven reagent consumption. This can result in transient shifts in amplification kinetics, potentially altering the shape of the amplification curve in inconsistent or irregular patterns. In addition, compared to dye-based LAMP, the relatively low fluorophore-probe concentration used in DARQ can increase the visibility of signal drift and optical noise, particularly in multiplex formats.

These factors, especially reduced primer concentrations and the intrinsic kinetics of DARQ chemistry, likely contribute to the extended threshold times observed in many multiplex assay reactions, often exceeding 30 min. While DARQ was chosen for its ability to enable target-specific fluorescence and multiplexing with minimal assay redesign, its inhibitory effect on amplification remains a limitation. Despite optimization of the QPD concentration relative to the supplemented primer, the sensitivity may not match that of the intercalating dye version of the assay(Crego-Vicente et al., 2023; Tanner et al., 2012; Zhang and Tanner, 2021). Strategies such as increasing polymerase concentration or using faster enzymes like NEB Bst 3.0 (or higher) may help improve reaction speed, although they carry a risk of non-specific amplification and require further optimization. Alternative probe-based methods, including molecular beacons(Sherrill-Mix et al., 2021), may offer better sensitivity but involve complex design considerations, such as matching melting temperatures for both the stem and target regions, and require screening of complementary target-specific sequences. Another approach involves probes that hybridize to specific regions of the LAMP amplicon, where fluorescence is generated upon probe linearization, and incorporating locked nucleic acid (LNA) bases can improve probe stability and simplify design(Zhang and Tanner, 2022). These alternative strategies may serve as viable options for future assay development aimed at improving sensitivity, speed, or ease of multiplexing beyond the current DARQ-based implementation.

Employing the multiplex RT-LAMP in a single-pot format for testing multiple RNA targets demonstrated the assay's robustness and adaptability, which aligns with the emerging need for flexible diagnostic platforms capable of simultaneously detecting and distinguishing multiple pathogens. Our results demonstrate that the assay can qualitatively detect viral RNAs, aligning well with the performance of standard RT-PCR and confirming its practical utility. An aspect not explored in this study is the quantitative analysis during multiplexing, which is limited by insufficient sensitivity and could impede the detection of low viral loads. Future studies should, therefore, focus on investigating the kinetic impacts of multiplexing in RT-LAMP assays, such as how the presence and concentration of one target influence the detection of another. Additionally, it is essential to explore methods to enhance the quantitative capabilities of these assays, thereby improving their ability to accurately measure viral loads and integrate minimal sample preparation steps, particularly for saliva (Tang et al., 2022), which could extend the assay's applicability to more routine diagnostic use.

This study contributes to the ongoing development of molecular diagnostics by enhancing the flexibility and specificity of multiplex RT-LAMP assays. The ability to maintain specificity while testing for multiple pathogens in a single assay setup could position this approach as a practical tool in outbreak management and disease surveillance with simple-to-obtain samples that can improve compliance. Enhancements in assay sensitivity and integration of streamlined sample preparation methods will further the practical application of this technology. Our findings lay the groundwork for future innovations in point-of-need diagnostics, promising improved healthcare outcomes through early and precise pathogen detection.

5. Conclusion

In this work, we developed a multiplexed diagnostic test designed to detect SARS-CoV-2, Flu-A, and RSV RNA from non-invasive saliva samples, directly addressing the challenge of distinguishing between respiratory viral infections with overlapping symptoms at the point of need. By training a neural network on calibration data, our system estimates time-varying fluorophore concentrations in a one-pot triplex RT-LAMP reaction, eliminating the need for specialized optical filters and simplifying the hardware design while enabling target discrimination. The analyzer successfully identified mock saliva samples representing single or dual viral infections, demonstrating practical performance comparable to standard RT-PCR. Future directions include refining primer designs and assay conditions to enable quantitative analysis, improving the detection limit, and studying how the presence or concentration of one target may influence the amplification kinetics of others in multiplexed RT-LAMP assays. Refinements to the fluorophore concentration prediction model that incorporate the combined behavior of fluorophores based on their independent calibration data may reduce the need for combinatorial experiments, further improving the scalability of the approach. This study lays a foundation for flexible molecular diagnostics using simple saliva samples and compact instrumentation, supporting real-time detection of multiple respiratory pathogens in decentralized settings.

CRediT authorship contribution statement

Aneesh Kshirsagar: Writing – review & editing, Writing – original draft, Visualization, Validation, Software, Methodology, Investigation, Formal analysis, Data curation, Conceptualization. **Dean DeRosa:** Software, Investigation. **Anthony J. Politza:** Writing – review & editing, Visualization, Investigation, Formal analysis. **Tianyi Liu:** Visualization, Methodology. **Ming Dong:** Writing – review & editing, Visualization, Supervision, Methodology. **Weihua Guan:** Writing – review & editing, Visualization, Supervision, Resources, Project administration, Funding acquisition, Conceptualization.

Declaration of generative AI and AI-assisted technologies in the writing process

During the preparation of this work, the authors used ChatGPT (powered by OpenAI's language model, GPT-4; http://openai.com) in order to refine the manuscript text for grammatical correctness and to improve readability. After using this tool/service, the author(s) reviewed and edited the content as needed and take full responsibility for the content of the publication.

Declaration of competing interest

The authors declare that they have no known competing financial interests or personal relationships that could have appeared to influence the work reported in this paper.

Acknowledgments

This work was partially supported by the National Institutes of Health (R61AI147419, R33AI147419, R33HD105610), the National Science Foundation (2319913), and the American Rescue Plan Act through USDA APHIS (APHIS/NIFA Collaborative award# 2023-70432-41395). Any opinions, findings, conclusions, or recommendations expressed in this work are those of the authors and should not be construed to represent any official NSF, NIH, USDA, or US Government determination or policy.

Appendix A. Supplementary data

Supplementary data to this article can be found online at https://doi.org/10.1016/j.bios.2025.117836.

Data availability

Data will be made available on request.

References

Ackerman, C.M., Myhrvold, C., Thakku, S.G., Freije, C.A., Metsky, H.C., Yang, D.K., Ye, S. H., Boehm, C.K., Kosoko-Thoroddsen, T.-S.F., Kehe, J., Nguyen, T.G., Carter, A., Kulesa, A., Barnes, J.R., Dugan, V.G., Hung, D.T., Blainey, P.C., Sabeti, P.C., 2020. Massively multiplexed nucleic acid detection with Cas13. Nature 582, 277–282. https://doi.org/10.1038/s41586-020-2279-8.

Aptitude Medical Systems, 2025. Aptitude Metrix Covid/Flu test [WWW Document]. https://cdn.prod.website-files.com/62ec1fa0e73b133056658278/67e593a1dea4b30820a39aca_03-C_F-IFU.pdf, 7.2.25.

Arons, M.M., Hatfield, K.M., Reddy, S.C., Kimball, A., James, A., Jacobs, J.R., Taylor, J., Spicer, K., Bardossy, A.C., Oakley, L.P., Tanwar, S., Dyal, J.W., Harney, J., Chisty, Z., Bell, J.M., Methner, M., Paul, P., Carlson, C.M., McLaughlin, H.P., Thornburg, N., Tong, S., Tamin, A., Tao, Y., Uehara, A., Harcourt, J., Clark, S., Brostrom-Smith, C., Page, L.C., Kay, M., Lewis, J., Montgomery, P., Stone, N.D., Clark, T.A., Honein, M. A., Duchin, J.S., Jernigan, J.A., 2020. Presymptomatic SARS-CoV-2 infections and transmission in a skilled nursing facility. N. Engl. J. Med. 382, 2081–2090. https://doi.org/10.1056/NEJMoa2008457.

Ball, C.S., Light, Y.K., Koh, C.-Y., Wheeler, S.S., Coffey, L.L., Meagher, R.J., 2016. Quenching of unincorporated amplification signal reporters in reverse-transcription loop-mediated isothermal amplification enabling bright, single-step, closed-tube, and multiplexed detection of RNA viruses. Anal. Chem. 88, 3562–3568. https://doi.org/10.1021/acs.analchem.5b04054.

Bartlow, A.W., Stromberg, Z.R., Gleasner, C.D., Hu, B., Davenport, K.W., Jakhar, S., Li, P.-E., Vosburg, M., Garimella, M., Chain, P.S.G., Erkkila, T.H., Fair, J.M., Mukundan, H., 2022. Comparing variability in diagnosis of upper respiratory tract infections in patients using syndromic, next generation sequencing, and PCR-Based methods. PLOS Glob. Public Health 2, e0000811. https://doi.org/10.1371/journal.pgph.0000811.

Behrmann, O., Bachmann, I., Spiegel, M., Schramm, M., Abd El Wahed, A., Dobler, G., Dame, G., Hufert, F.T., 2020. Rapid detection of SARS-CoV-2 by low volume real-time single tube reverse transcription recombinase polymerase amplification using an exo probe with an internally linked quencher (Exo-IQ). Clin. Chem. 66, 1047–1054. https://doi.org/10.1093/clinchem/hvaa116.

Beigel, J.H., Tomashek, K.M., Dodd, L.E., Mehta, A.K., Zingman, B.S., Kalil, A.C., Hohmann, E., Chu, H.Y., Luetkemeyer, A., Kline, S., Castilla, D.L. de, Finberg, R.W., Dierberg, K., Tapson, V., Hsieh, L., Patterson, T.F., Paredes, R., Sweeney, D.A., Short, W.R., Touloumi, G., Lye, D.C., Ohmagari, N., Oh, M., Ruiz-Palacios, G.M., Benfield, T., Fätkenheuer, G., Kortepeter, M.G., Atmar, R.L., Creech, C.B., Lundgren, J., Babiker, A.G., Pett, S., Neaton, J.D., Burgess, T.H., Bonnett, T., Green, M., Makowski, M., Osinusi, A., Nayak, S., Lane, H.C., 2020. Remdesivir for the treatment of Covid-19 — final report. N. Engl. J. Med. 383, 1813–1826. https://doi.org/10.1056/NEJMoa2007764.

Berry, G.J., Zhen, W., Smith, E., Manji, R., Silbert, S., Lima, A., Harington, A., McKinley, K., Kensinger, B., Neff, C., Lu, D., 2022. Multicenter evaluation of the BioFire respiratory panel 2.1 (RP2.1) for detection of SARS-CoV-2 in nasopharyngeal swab samples. J. Clin. Microbiol. 60, e0006622. https://doi.org/10.1128/jcm.00066-22.

Blumenfeld, N.R., Bolene, M.A.E., Jaspan, M., Ayers, A.G., Zarrandikoetxea, S., Freudman, J., Shah, N., Tolwani, A.M., Hu, Y., Chern, T.L., Rogot, J., Behnam, V., Sekhar, A., Liu, X., Onalir, B., Kasumi, R., Sanogo, A., Human, K., Murakami, K., Totapally, G.S., Fasciano, M., Sia, S.K., 2022. Multiplexed reverse-transcriptase quantitative polymerase chain reaction using plasmonic nanoparticles for point-of-care COVID-19 diagnosis. Nat. Nanotechnol. 17, 984–992. https://doi.org/10.1038/s41565-022-01175-4.

Broughton, J.P., Deng, X., Yu, G., Fasching, C.L., Servellita, V., Singh, J., Miao, X., Streithorst, J.A., Granados, A., Sotomayor-Gonzalez, A., Zorn, K., Gopez, A., Hsu, E., Gu, W., Miller, S., Pan, C.-Y., Guevara, H., Wadford, D.A., Chen, J.S., Chiu, C.Y., 2020. CRISPR–Cas12-based detection of SARS-CoV-2. Nat. Biotechnol. 38, 870–874. https://doi.org/10.1038/s41587-020-0513-4.

CDC, 2023. Symptoms and Care for RSV [WWW Document]. Cent. Dis. Control Prev. https://www.cdc.gov/rsv/about/symptoms.html, 1.4.24.

Crego-Vicente, B., Fernández-Soto, P., García-Bernalt Diego, J., Febrer-Sendra, B., Muro, A., 2023. Development of a duplex LAMP assay with probe-based readout for simultaneous real-time detection of Schistosoma mansoni and strongyloides spp. -A laboratory approach to point-of-care. Int. J. Mol. Sci. 24, 893. https://doi.org/10.3390/ijms24010893.

Cuadrado-Payán, E., Montagud-Marrahi, E., Torres-Elorza, M., Bodro, M., Blasco, M., Poch, E., Soriano, A., Piñeiro, G.J., 2020. SARS-CoV-2 and influenza virus co-infection. Lancet 395, e84. https://doi.org/10.1016/S0140-6736(20)31052-7.

Dai, F., Zhang, T., Pang, F., Jiao, T., Wang, K., Zhang, Z., Wang, N., Xie, Z., Zhang, Y., Wang, Z., Chen, Z., Yu, M., Wei, H., Song, J., 2025. A compact, palm-sized isothermal fluorescent diagnostic intelligent IoT device for personal health monitoring and beyond via one-tube/one-step LAMP-CRISPR assay. Biosens. Bioelectron. 270, 116945. https://doi.org/10.1016/j.bios.2024.116945.

Dewhurst, R.E., Heinrich, T., Watt, P., Ostergaard, P., Marimon, J.M., Moreira, M., Houldsworth, P.E., Rudrum, J.D., Wood, D., Kōks, S., 2022. Validation of a rapid, saliva-based, and ultra-sensitive SARS-CoV-2 screening system for pandemic-scale infection surveillance. Sci. Rep. 12, 5936. https://doi.org/10.1038/s41598-022-08263-4.

Diagenetix, Inc., 2025. Bioranger [WWW Document]. shop.diagenetix.com. https://shop.diagenetix.com/product-p/sd.v.3.0.htm, 7.3.25.

Ding, Q., Lu, P., Fan, Y., Xia, Y., Liu, M., 2020. The clinical characteristics of pneumonia patients coinfected with 2019 novel coronavirus and influenza virus in wuhan, China. J. Med. Virol. 92, 1549–1555. https://doi.org/10.1002/jmv.25781.

Dong, Y., Zhao, Y., Li, S., Wan, Z., Lu, R., Yang, X., Yu, G., Reboud, J., Cooper, J.M., Tian, Z., Zhang, C., 2022. Multiplex, real-time, point-of-care RT-LAMP for SARS-CoV-2 detection using the HFman probe. ACS Sens. 7, 730–739. https://doi.org/10.1021/acssensors.1c02079.

Faruque, M.R.J., Bikker, F.J., Laine, M.L., 2023. Comparing SARS-CoV-2 viral load in human saliva to oropharyngeal swabs, nasopharyngeal swabs, and sputum: a systematic review and meta-analysis. Can. J. Infect. Dis. Med. Microbiol. J. Can. Mal. Infect. Microbiol. Médicale, 5807370. https://doi.org/10.1155/2023/5807370, 2023.

Fischer, W.A., Eron, J.J., Holman, W., Cohen, M.S., Fang, L., Szewczyk, L.J., Sheahan, T. P., Baric, R., Mollan, K.R., Wolfe, C.R., Duke, E.R., Azizad, M.M., Borroto-Esoda, K., Wohl, D.A., Coombs, R.W., James Loftis, A., Alabanza, P., Lipansky, F., Painter, W.P., 2021. A phase 2a clinical trial of molnupiravir in patients with COVID-19 shows accelerated SARS-CoV-2 RNA clearance and elimination of infectious virus. Sci. Transl. Med. 14, eabl7430. https://doi.org/10.1126/scitranslmed.abl7430.

Food and Drug Administration, 2024. COVID-19 the Cue COVID-19 Test for Home and over the Counter (OTC) Use Instructions for Use [WWW Document]. https://www.fda.gov/media/146470/download, 7.2.25.

Furlow, B., 2023. Triple-demic overwhelms paediatric units in US hospitals. Lancet Child Adolesc. Health 7, 86. https://doi.org/10.1016/S2352-4642(22)00372-8.

Gagnon, F., Bhatt, M., Zemek, R., Webster, R.J., Johnson-Obaseki, S., Harman, S., 2022. Nasopharyngeal swabs vs. saliva sampling for SARS-CoV-2 detection: a cross-sectional survey of acceptability for caregivers and children after experiencing both methods. PLoS One 17, e0270929. https://doi.org/10.1371/journal.pone.0270929.

Galar, A., Catalán, P., Vesperinas, L., Miguens, I., Muñoz, I., García-Espona, A., Sevillano, J.A., Andueza, J.A., Bouza, E., Muñoz, P., 2021. Use of saliva swab for detection of influenza virus in patients admitted to an emergency department. Microbiol. Spectr. 9. https://doi.org/10.1128/spectrum.00336-21.

Gootenberg, J.S., Abudayyeh, O.O., Lee, J.W., Essletzbichler, P., Dy, A.J., Joung, J., Verdine, V., Donghia, N., Daringer, N.M., Freije, C.A., Myhrvold, C., Bhattacharyya, R.P., Livny, J., Regev, A., Koonin, E.V., Hung, D.T., Sabeti, P.C., Collins, J.J., Zhang, F., 2017. Nucleic acid detection with CRISPR-Cas13a/C2c2. Science 356, 438–442. https://doi.org/10.1126/science.aam9321.

Gottlieb, R.L., Vaca, C.E., Paredes, R., Mera, J., Webb, B.J., Perez, G., Oguchi, G., Ryan, P., Nielsen, B.U., Brown, M., Hidalgo, A., Sachdeva, Y., Mittal, S., Osiyemi, O., Skarbinski, J., Juneja, K., Hyland, R.H., Osinusi, A., Chen, S., Camus, G., Abdelghany, M., Davies, S., Behenna-Renton, N., Duff, F., Marty, F.M., Katz, M.J., Ginde, A.A., Brown, S.M., Schiffer, J.T., Hill, J.A., 2022. Early remdesivir to prevent progression to severe Covid-19 in outpatients. N. Engl. J. Med. 386, 305–315. https://doi.org/10.1056/NEJMoa2116846.

Hardinge, P., Murray, J.A.H., 2019. Reduced false positives and improved reporting of loop-mediated isothermal amplification using quenched fluorescent primers. Sci. Rep. 9, 7400. https://doi.org/10.1038/s41598-019-43817-z.

Jarrett, J., Uhteg, K., Forman, M.S., Hanlon, A., Vargas, C., Carroll, K.C., Valsamakis, A., Mostafa, H.H., 2021. Clinical performance of the GenMark Dx ePlex respiratory pathogen panels for upper and lower respiratory tract infections. J. Clin. Virol. 135, 104737. https://doi.org/10.1016/j.jcv.2021.104737.

Kim, D.H., Kim, D., Moon, J.W., Chae, S.-W., Rhyu, I.J., 2022. Complications of nasopharyngeal swabs and safe procedures for COVID-19 testing based on anatomical knowledge. J. Kor. Med. Sci. 37, e88. https://doi.org/10.3346/jkms.2022.37.e88.

Kim, Y., Yun, S.G., Kim, M.Y., Park, K., Cho, C.H., Yoon, S.Y., Nam, M.H., Lee, C.K., Cho, Y.-J., Lim, C.S., 2016. Comparison between saliva and nasopharyngeal swab specimens for detection of respiratory viruses by multiplex reverse Transcription-PCR. J. Clin. Microbiol. 55, 226–233. https://doi.org/10.1128/jcm.01704-16.

Kshirsagar, A., Choi, G., Santosh, V., Harvey, T., Bernhards, R.C., Guan, W., 2023. Handheld purification-free nucleic acid testing device for point-of-need detection of malaria from whole blood. ACS Sens. 8, 673–683. https://doi.org/10.1021/acssensors.2c02169.

Kshirsagar, A., Politza, A.J., Guan, W., 2024. Deep learning enabled universal multiplexed fluorescence detection for point-of-care applications. ACS Sens. 9, 4017–4027. https://doi.org/10.1021/acssensors.4c00860.

Kudo, E., Israelow, B., Vogels, C.B.F., Lu, P., Wyllie, A.L., Tokuyama, M., Venkataraman, A., Brackney, D.E., Ott, I.M., Petrone, M.E., Earnest, R., Lapidus, S., Muenker, M.C., Moore, A.J., Casanovas-Massana, A., Team, Y.I.R., Omer, S.B., Cruz, C.S.D., Farhadian, S.F., Ko, A.I., Grubaugh, N.D., Iwasaki, A., 2020. Detection of SARS-CoV-2 RNA by multiplex RT-qPCR. PLoS Biol. 18, e3000867. https://doi.org/10.1371/journal.pbio.3000867.

Kundrod, K.A., Natoli, M.E., Chang, M.M., Smith, C.A., Paul, S., Ogoe, D., Goh, C., Santhanaraj, A., Price, A., Eldin, K.W., Patel, K.P., Baker, E., Schmeler, K.M., Richards-Kortum, R., 2022. Sample-to-answer, extraction-free, real-time RT-LAMP test for SARS-CoV-2 in nasopharyngeal, nasal, and saliva samples: implications and use for surveillance testing. PLoS One 17, e0264130. https://doi.org/10.1371/journal.pone.0264130.

Lalli, M.A., Langmade, J.S., Chen, X., Fronick, C.C., Sawyer, C.S., Burcea, L.C., Wilkinson, M.N., Fulton, R.S., Heinz, M., Buchser, W.J., Head, R.D., Mitra, R.D., Milbrandt, J., 2021. Rapid and extraction-free detection of SARS-CoV-2 from saliva by colorimetric reverse-transcription loop-mediated isothermal amplification. Clin. Chem. 67, 415–424. https://doi.org/10.1093/clinchem/hvaa267.

Lansbury, L., Lim, B., Baskaran, V., Lim, W.S., 2020. Co-infections in people with COVID-19: a systematic review and meta-analysis. J. Infect. 81, 266–275. https://doi.org/10.1016/j.jinf.2020.05.046.

Leung, E.C., Chow, V.C., Lee, M.K., Tang, K.P., Li, D.K., Lai, R.W., 2021. Evaluation of the xpert xpress SARS-CoV-2/Flu/RSV assay for simultaneous detection of SARS-CoV-2, influenza A and B viruses, and respiratory syncytial virus in nasopharyngeal specimens. J. Clin. Microbiol. 59. https://doi.org/10.1128/jcm.02965-20.

Li, Z., Bruce, J.L., Cohen, B., Cunningham, C.V., Jack, W.E., Kunin, K., Langhorst, B.W., Miller, J., Moncion, R.A., Poole, C.B., Premsrirut, P.K., Ren, G., Roberts, R.J., Tanner, N.A., Zhang, Y., Carlow, C.K.S., 2022. Development and implementation of a simple and rapid extraction-free saliva SARS-CoV-2 RT-LAMP workflow for workplace surveillance. PLoS One 17, e0268692. https://doi.org/10.1371/journal.pone.0268692.

Liu, T., Choi, G., Tang, Z., Kshirsagar, A., Politza, A.J., Guan, W., 2022. Fingerpick blood-based nucleic acid testing on A USB interfaced device towards HIV self-testing. Biosens. Bioelectron. 209, 114255. https://doi.org/10.1016/j.bios.2022.114255.

Ludwig, K.U., Schmithausen, R.M., Li, D., Jacobs, M.L., Hollstein, R., Blumenstock, K., Liebing, J., Słabicki, M., Ben-Shmuel, A., Israeli, O., Weiss, S., Ebert, T.S., Paran, N., Rüdiger, W., Wilbring, G., Feldman, D., Lippke, B., Ishorst, N., Hochfeld, L.M., Beins, E.C., Kaltheuner, I.H., Schmitz, M., Wöhler, A., Döhla, M., Sib, E., Jentzsch, M., Moench, E.-M.C., Borrajo, J.D., Strecker, J., Reinhardt, J., Cleary, B., Geyer, M., Hölzel, M., Macrae, R., Nöthen, M.M., Hoffmann, P., Exner, M., Regev, A., Zhang, F., Schmid-Burgk, J.L., 2021. LAMP-seq enables sensitive, multiplexed COVID-19 diagnostics using molecular barcoding. Nat. Biotechnol. 39, 1556–1562. https://doi.org/10.1038/s41587-021-00966-9.

Mullis, K.B., Faloona, F.A., 1987. Specific synthesis of DNA *In vitro* via a polymerase-catalyzed chain reaction. In: Methods in Enzymology, Recombinant DNA Part F. Academic Press, pp. 335–350. https://doi.org/10.1016/0076-6879(87)55023-6.

Ngaosuwankul, N., Noisumdaeng, P., Komolsiri, P., Pooruk, P., Chokephaibulkit, K., Chotpitayasunondh, T., Sangsajja, C., Chuchottaworn, C., Farrar, J., Puthavathana, P., 2010. Influenza A viral loads in respiratory samples collected from patients infected with pandemic H1N1, seasonal H1N1 and H3N2 viruses. Virol. J. 7, 75. https://doi.org/10.1186/1743-422X-7-75.

Notomi, T., Okayama, H., Masubuchi, H., Yonekawa, T., Watanabe, K., Amino, N., Hase, T., 2000. Loop-mediated isothermal amplification of DNA. Nucleic Acids Res. 28, e63. https://doi.org/10.1093/nar/28.12.e63.

Olsen, S.J., 2021. Changes in influenza and other respiratory virus activity during the COVID-19 pandemic — united States, 2020–2021. MMWR Morb. Mortal. Wkly. Rep. 70. https://doi.org/10.15585/mmwr.mm7029a1.

Ott, I.M., Strine, M.S., Watkins, A.E., Boot, M., Kalinich, C.C., Harden, C.A., Vogels, C.B. F., Casanovas-Massana, A., Moore, A.J., Muenker, M.C., Nakahata, M., Tokuyama, M., Nelson, A., Fournier, J., Bermejo, S., Campbell, M., Datta, R., Dela Cruz, C.S., Farhadian, S.F., Ko, A.I., Iwasaki, A., Grubaugh, N.D., Wilen, C.B., Wyllie, A.L., the Yale IMPACT Research team3, 2021. Stability of SARS-CoV-2 RNA in nonsupplemented saliva. Emerg. Infect. Dis. 27, 1146–1150. https://doi.org/10.3201/eid2704.204199.

Owen, D.R., Allerton, C.M.N., Anderson, A.S., Aschenbrenner, L., Avery, M., Berritt, S., Boras, B., Cardin, R.D., Carlo, A., Coffman, K.J., Dantonio, A., Di, L., Eng, H., Ferre, R., Gajiwala, K.S., Gibson, S.A., Greasley, S.E., Hurst, B.L., Kadar, E.P., Kalgutkar, A.S., Lee, J.C., Lee, J., Liu, W., Mason, S.W., Noell, S., Novak, J.J., Obach, R.S., Ogilvie, K., Patel, N.C., Pettersson, M., Rai, D.K., Reese, M.R., Sammons, M.F., Sathish, J.G., Singh, R.S.P., Steppan, C.M., Stewart, A.E., Tuttle, J. B., Updyke, L., Verhoest, P.R., Wei, L., Yang, Q., Zhu, Y., 2021. An oral SARS-CoV-2 M^{pro} inhibitor clinical candidate for the treatment of COVID-19. Science 374, 1586–1593. https://doi.org/10.1126/science.abl4784.

Peci, A., Tran, V., Guthrie, J.L., Li, Y., Nelson, P., Schwartz, K.L., Eshaghi, A., Buchan, S. A., Gubbay, J.B., 2021. Prevalence of Co-Infections with respiratory viruses in individuals investigated for SARS-CoV-2 in Ontario, Canada. Viruses 13, 130. https://doi.org/10.3390/v13010130.

Perkins, S.M., Webb, D.L., Torrance, S.A., El Saleeby, C., Harrison, L.M., Aitken, J.A., Patel, A., DeVincenzo, J.P., 2005. Comparison of a real-time reverse transcriptase PCR assay and a culture technique for quantitative assessment of viral load in children naturally infected with respiratory syncytial virus. J. Clin. Microbiol. 43, 2356–2362. https://doi.org/10.1128/JCM.43.5.2356-2362.2005.

Pfizer Inc., 2023. LUCIRA® by Pfizer for COVID-19 & Flu at Home Test [WWW Document]. https://www.lucirabypfizer.com/, 1.1.24.

Piepenburg, O., Williams, C.H., Stemple, D.L., Armes, N.A., 2006. DNA detection using recombination proteins. PLoS Biol. 4, e204. https://doi.org/10.1371/journal.pbio.0040204.

Politza, A.J., Liu, T., Guan, W., 2023. Programmable magnetic robot (ProMagBot) for automated nucleic acid extraction at the point of need. Lab Chip 23, 3882–3892. https://doi.org/10.1039/D3LC00545C.

Politza, A.J., Liu, T., Kshirsagar, A., Dong, M., Ahamed, Md. A., Guan, W., 2024. Development and validation of a portable device for lab-free versatile nucleic acid extraction. BioTechniques 76 (10), 505–515. https://doi.org/10.1080/07366205.2024.2427544.

Robinson, J.L., Lee, B.E., Kothapalli, S., Craig, W.R., Fox, J.D., 2008. Use of throat swab or saliva specimens for detection of respiratory viruses in children. Clin. Infect. Dis. 46, e61–e64. https://doi.org/10.1086/529386.

Rombach, M., Hin, S., Specht, M., Johannsen, B., Lüddecke, J., Paust, N., Zengerle, R., Roux, L., Sutcliffe, T., R Peham, J., Herz, C., Panning, M., Mantke, O.D., Mitsakakis, K., 2020. RespiDisk: a point-of-care platform for fully automated detection of respiratory tract infection pathogens in clinical samples. Analyst 145, 7040–7047. https://doi.org/10.1039/D0AN01226B.

Sherrill-Mix, S., Hwang, Y., Roche, A.M., Glascock, A., Weiss, S.R., Li, Y., Haddad, L., Deraska, P., Monahan, C., Kromer, A., Graham-Wooten, J., Taylor, L.J., Abella, B.S., Ganguly, A., Collman, R.G., Van Duyne, G.D., Bushman, F.D., 2021. Detection of SARS-CoV-2 RNA using RT-LAMP and molecular beacons. Genome Biol. 22, 169. https://doi.org/10.1186/s13059-021-02387-y.

Stiver, G., 2003. The treatment of influenza with antiviral drugs. CMAJ Can. Med. Assoc. J. 168, 49–57.

Takayama, I., Nakauchi, M., Takahashi, H., Oba, K., Semba, S., Kaida, A., Kubo, H., Saito, S., Nagata, S., Odagiri, T., Kageyama, T., 2019. Development of real-time fluorescent reverse transcription loop-mediated isothermal amplification assay with quenching primer for influenza virus and respiratory syncytial virus. J. Virol. Methods 267, 53–58. https://doi.org/10.1016/j.jviromet.2019.02.010.

Tang, Z., Cui, J., Kshirsagar, A., Liu, T., Yon, M., Kuchipudi, S.V., Guan, W., 2022. SLIDE: saliva-based SARS-CoV-2 self-testing with RT-LAMP in a mobile device. ACS Sens. 7, 2370–2378. https://doi.org/10.1021/acssensors.2c01023.

Tanner, N.A., Zhang, Y., Evans, T.C., 2012. Simultaneous multiple target detection in real-time loop-mediated isothermal amplification. Biotechniques 53, 81–89. https://doi.org/10.2144/0000113902.

To, K.K., Lu, L., Yip, C.C., Poon, R.W., Fung, A.M., Cheng, A., Yuen, K.Y., 2017. Additional molecular testing of saliva specimens improves the detection of respiratory viruses. Emerging Microbes & Infections 6 (1), 1–7. https://doi.org/10.1038/emi.2017.35.

Trick, A.Y., Chen, F.-E., Chen, L., Lee, P.-W., Hasnain, A.C., Mostafa, H.H., Carroll, K.C., Wang, T.-H., 2022. Point-of-Care platform for rapid multiplexed detection of SARS-CoV-2 variants and respiratory pathogens. Adv. Mater. Technol. 7, 2101013. https://doi.org/10.1002/admt.202101013.

Vincent, M., Xu, Y., Kong, H., 2004. Helicase-dependent isothermal DNA amplification. EMBO Rep. 5, 795–800. https://doi.org/10.1038/sj.embor.7400200.

Visby Medical, 2025. Respiratory Health Test — POC Rapid PCR Device | Visby Medical. Visby Med. https://www.visbymedical.com/respiratory-health-test/, 7.2.25.

Vogels, C.B.F., Watkins, A.E., Harden, C.A., Brackney, D.E., Shafer, J., Wang, J., Caraballo, C., Kalinich, C.C., Ott, I.M., Fauver, J.R., Kudo, E., Lu, P., Venkataraman, A., Tokuyama, M., Moore, A.J., Muenker, M.C., Casanovas-Massana, A., Fournier, J., Bermejo, S., Campbell, M., Datta, R., Nelson, A., Anastasio, K., Askenase, M.H., Batsu, M., Bickerton, S., Brower, K., Bucklin, M.L., Cahill, S., Cao, Y., Courchaine, E., DeIuliis, G., Earnest, R., Geng, B., Goldman-Israelow, B., Handoko, R., Khoury-Hanold, W., Kim, D., Knaggs, L., Kuang, M., Lapidus, S., Lim, J., Linehan, M., Lu-Culligan, A., Martin, A., Matos, I., McDonald, D., Minasyan, M., Nakahata, M., Naushad, N., Nouws, J., Obaid, A., Odio, C., Oh, J.E., Omer, S., Park, A., Park, H.-J., Peng, X., Petrone, M., Prophet, S., Rice, T., Rose, K.-A., Sewanan, L., Sharma, L., Shaw, A.C., Shepard, D., Smolgovsky, M., Sonnert, N., Strong, Y., Todeasa, C., Valdez, J., Velazquez, S., Vijayakumar, P., White, E.B., Yang, Y., Cruz, C.S.D., Ko, A.I., Iwasaki, A., Krumholz, H.M., Matheus, J.D., Hui, P., Liu, C., Farhadian, S.F., Sikka, R., Wyllie, A.L., Grubaugh, N.D., 2021. SalivaDirect: a simplified and flexible platform to enhance SARS-CoV-2 testing capacity. Med 2, 263–280. https://doi.org/10.1016/j.medj.2020.12.010 e6.

Wyllie, A.L., Fournier, J., Casanovas-Massana, A., Campbell, M., Tokuyama, M., Vijayakumar, P., Warren, J.L., Geng, B., Muenker, M.C., Moore, A.J., Vogels, C.B.F., Petrone, M.E., Ott, I.M., Lu, P., Venkataraman, A., Lu-Culligan, A., Klein, J., Earnest, R., Simonov, M., Datta, R., Handoko, R., Naushad, N., Sewanan, L.R., Valdez, J., White, E.B., Lapidus, S., Kalinich, C.C., Jiang, X., Kim, D.J., Kudo, E., Linehan, M., Mao, T., Moriyama, M., Oh, J.E., Park, A., Silva, J., Song, E., Takahashi, T., Taura, M., Weizman, O.-E., Wong, P., Yang, Y., Bermejo, S., Odio, C. D., Omer, S.B., Cruz, C.S.D., Farhadian, S., Martinello, R.A., Iwasaki, A., Grubaugh, N.D., Ko, A.I., 2020. Saliva or nasopharyngeal swab specimens for detection of SARS-CoV-2. N. Engl. J. Med. 383, 1283–1286. https://doi.org/10.1056/NEJMc2016359.

Xun, G., Lane, S.T., Petrov, V.A., Pepa, B.E., Zhao, H., 2021. A rapid, accurate, scalable, and portable testing system for COVID-19 diagnosis. Nat. Commun. 12, 2905. https://doi.org/10.1038/s41467-021-23185-x.

Yang, J., Gong, Y., Zhang, C., Sun, J., Wong, G., Shi, W., Liu, W., Gao, G.F., Bi, Y., 2022. Co-existence and co-infection of influenza A viruses and coronaviruses: public health challenges. Innovation 3, 100306. https://doi.org/10.1016/j.xinn.2022.100306.

Yeh, E.-C., Fu, C.-C., Hu, L., Thakur, R., Feng, J., Lee, L.P., 2017. Self-powered integrated microfluidic point-of-care low-cost enabling (SIMPLE) chip. Sci. Adv. 3, e1501645. https://doi.org/10.1126/sciadv.1501645.

Yoon, J., Yun, S.G., Nam, J., Choi, S.-H., Lim, C.S., 2017. The use of saliva specimens for detection of influenza A and B viruses by rapid influenza diagnostic tests. J. Virol. Methods 243, 15–19. https://doi.org/10.1016/j.jviromet.2017.01.013.

Yue, H., Zhang, M., Xing, L., Wang, K., Rao, X., Liu, H., Tian, J., Zhou, P., Deng, Y., Shang, J., 2020. The epidemiology and clinical characteristics of co-infection of SARS-CoV-2 and influenza viruses in patients during COVID-19 outbreak. J. Med. Virol. 92, 2870–2873. https://doi.org/10.1002/jmv.26163.

Zhang, C., Zheng, T., Wang, H., Chen, W., Huang, X., Liang, J., Qiu, L., Han, D., Tan, W., 2021. Rapid one-pot detection of SARS-CoV-2 based on a lateral flow assay in clinical samples. Anal. Chem. 93, 3325–3330. https://doi.org/10.1021/acs.analchem.0c05059.

Zhang, W.S., Pan, J., Li, F., Zhu, M., Xu, M., Zhu, H., Yu, Y., Su, G., 2021. Reverse transcription recombinase polymerase amplification coupled with CRISPR-Cas12a for facile and highly sensitive colorimetric SARS-CoV-2 detection. Anal. Chem. 93, 4126–4133. https://doi.org/10.1021/acs.analchem.1c00013.

Zhang, Y., Tanner, N.A., 2022. Efficient multiplexing and variant discrimination in reverse-transcription loop-mediated isothermal amplification with sequence-specific hybridization probes. Biotechniques 73, 235–243. https://doi.org/10.2144/btn-2022-0096.

Zhang, Y., Tanner, N.A., 2021. Development of multiplexed reverse-transcription loop-mediated isothermal amplification for detection of SARS-CoV-2 and influenza viral RNA. Biotechniques 70, 167–174. https://doi.org/10.2144/btn-2020-0157.